PLOS ONE

RESEARCH ARTICLE

SOX2 promotes a cancer stem cell-like phenotype and local spreading in oral squamous cell carcinoma

Alessandro Sacco[1☯], Anna Martina Battaglia[1☯], Gianluca Santamaria[1], Caterina Buffone[2], Selene Barone[2], Anna Procopio[3], Anna Maria Lavecchia[4], Ilenia Aversa[1], Emanuele Giorgio[1], Lavinia Petriaggi[1], Maria Giulia Cristofaro[1], Flavia Biamonte[1,5]*, Amerigo Giudice[2]

1 Department of Experimental and Clinical Medicine, Biochemistry and Molecular Biology Laboratory, "Magna Graecia" University of Catanzaro, Catanzaro, Italy, **2** Department of Health Sciences, School of Dentistry, "Magna Graecia" University of Catanzaro, Catanzaro, Italy, **3** Department of Experimental and Clinical Medicine, Biomechatronics Laboratory, "Magna Græcia" University of Catanzaro, Catanzaro, Italy, **4** Anatomical Pathology Unit, Pugliese-Ciaccio Hospital, Catanzaro, Italy, **5** Center of Interdepartmental Services (CIS), "Magna Graecia" University of Catanzaro, Catanzaro, Italy

☯ These authors contributed equally to this work.
* flavia.biamonte@unicz.it

Check for updates

OPEN ACCESS

Citation: Sacco A, Battaglia AM, Santamaria G, Buffone C, Barone S, Procopio A, et al. (2023) SOX2 promotes a cancer stem cell-like phenotype and local spreading in oral squamous cell carcinoma. PLoS ONE 18(12): e0293475. https://doi.org/10.1371/journal.pone.0293475

Editor: Afsheen Raza, Abu Dhabi University, UNITED ARAB EMIRATES

Received: April 12, 2023

Accepted: October 13, 2023

Published: December 14, 2023

Copyright: © 2023 Sacco et al. This is an open access article distributed under the terms of the Creative Commons Attribution License, which permits unrestricted use, distribution, and reproduction in any medium, provided the original author and source are credited.

Data Availability Statement: All relevant data are within the manuscript and its Supporting information files. All publicly accessed data are available on databases (TCGA URL: http://ualcan.path.uab.edu/cgi-bin/ualcan-res.pl; GEO accession number: GSE64216, GSE138206, GSE74530, GSE3799) described in methodology.

Funding: The authors received no specific funding for this work.

Competing interests: The authors have declared that no competing interests exist.

Abstract

Emerging evidence shows that oral squamous cell carcinoma (OSCC) invasiveness can be attributed to a small subpopulation of cancer stem cells (CSCs) in the bulk of the tumor. However, the presence of CSCs in the OSCC close resection margins is still poorly unexplored. Here, we found that *BMI1*, *CD44*, *SOX2*, *OCT4*, *UBE2C*, *CXCR4* CSCs marker genes are significantly upregulated, while *IGF1-R*, *KLF4*, *ALDH1A1*, *CD133*, *FAM3C* are downregulated in the tumor core *vs* healthy mucosa of 24 patients with OSCC. Among these, *SOX2* appears also upregulated in the tumor close margin *vs* healthy mucosa and this significantly correlates with tumor size and lymph node compromise. *In vitro* analyses in CAL27 and SCC15 tongue squamous cell carcinoma cell lines, show that *SOX2* transient knockdown i) promotes the mesenchymal-to-epithelial transition, ii) smooths the invasiveness, iii) attenuates the 3D tumor sphere-forming capacity, and iv) partially increases the sensitivity to cisplatin treatment. Overall, our study highlights that the OSCC close margins can retain CSC-specific markers. Notably, *SOX2* may represent a useful CSCs marker to predict a more aggressive phenotype and a suitable target to prevent local invasiveness.

Introduction

Oral squamous cell carcinoma (OSCC) accounts for more than 90% of head and neck cancers (HNSCC) [1,2]. Curative therapeutic approaches for OSCC include surgical resection, radiotherapy, and chemotherapy; however, according to the current clinical guidelines, surgery remains the conclusive treatment option for most patients [3–8]. One of the major concerns in the OSCC resection is sparing as much healthy tissue as possible to preserve vital functions and esthetics. At the same time, removing all malignant cells from the bulk of the tumor and

around it is mandatory to reduce the possibility of local recurrence [3,8–11]. Although many efforts in defining "safe" surgical margins outside tumor boundaries have been achieved, local recurrence still affects up to 45% of OSCC patients [12–14]. In this regard, we and others have recently observed that OSCC close margins may retain molecular alterations that, otherwise, result undetectable through conventional histopathological examination, thus making the definition of "safe" tumor margins even more complex [11,15,16].

Local recurrence has been associated with two concepts: the minimal residual disease and the "field cancerization". In the case of minimal residual disease, a small number of tumor cells, undetected by routine histopathology, remain in the margins upon surgery [17,18]. In the case of "field cancerization", instead, a not macroscopically visible precancerous area surrounding the tumor stays behind unnoticed or can be detected as epithelial dysplasia [19,20]. Recently, the precancerous fields have been defined by the existence of genetic changes, either mutations, loss of heterozygosity (LOH), or copy number alterations (i.e., p53, CDKN2A, etc) [21–23]. However, the current detection methods of precancerous fields suffer from the problem of "undersampling", as only a very small number of residual cancer cells are present in a relatively large tissue volume. Therefore, the identification of this small cell subpopulation, which likely represents the foci of precancerous initiation and progression, represents a major concern in oral cancer research.

The persistence of a very small fraction of cancer cells, defined as cancer stem cells (CSCs), provided with high tumorigenic proficiency, motility, invasion, and drug resistance, is largely considered a primary cause of tumor recurrence [24–27]. During the last decade, a few CSCs-related genes have been identified in OSCC lesions and associated, even often contradictorily, with nodal metastasis, chemoresistance, tumor recurrence, and survival rate of OSCC patients [25,28,29]. Among these, *SOX2* has been found overexpressed along the different stages of oral carcinogenesis, from potentially malignant oral disorders to invasive carcinomas [30]. SOX2, a member of the SOX family of high-mobility group transcriptional factors, holds a pivotal role in embryonic development and the preservation of stemness features in both embryonic and adult stem cell populations [29]. Robust evidence derived from preclinical studies involving both cell cultures and genetically modified mouse models strongly supports the role of SOX2 as an oncogene. SOX2, indeed, crosstalks with multiple signaling pathways to tightly regulate critical biological processes associated with tumor initiation and progression, such as cell-cycle, apoptosis, autophagy, and epithelial-to-mesenchymal transition (EMT). Dysregulation of SOX2 expression and activity occurs in several cancer types and often correlates with advanced tumor stages, unfavorable prognosis, and drug resistance [31].

The expression-based and the functional-based characterization of CSCs, as well as their spatial organization within the tumor mass and the surrounding tumor microenvironment (TME), is an attractive field of investigation as it may provide remarkable information on the existence of pre-metastatic niches.

In this study, we analyzed the expression-based distribution of CSCs within the bulk of the oral tumor and their close margin. To this, we analyzed the gene expression profile of CSCs markers and its potential impact on tumor recurrence and prognosis. Then, we assessed the functional role of putative CSCs markers in the OSCC cell phenotype *in vitro*.

Results

SOX2 is overexpressed in the tumor core and its close margin of OSCC patients with lymph node compromise

According to previous findings of our [11] and other research groups (GEO databases, S1 Table) 13 CSCs markers genes (*BMI1*, *CD44*, *SOX2*, *OCT4*, *UBE2C*, *FAM3C*, *CXCR4*,

NANOG, *RRM2*, *IGF-1R*, *KLF4*, *ALDH1A*, *CD133*) are differentially expressed in OSCC tissues compared to the relative healthy mucosa. Hence, to assess the distribution of tumor cells with CSCs-like phenotype in OSCC core and close margins, we performed the gene expression profile of these 13 CSCs markers in three different tissue samples (tumor core (T), tumor-free close margin (CM) and adjacent health distant margin (DM)) collected from a cohort of 24 patients with histologically confirmed OSCC. Clinicopathological, as well as demographic characteristics of the 24 patients enrolled in this study, are presented in Table 1.

Briefly, the mean age of patients at recruitment was 68.6; the 58.3% was composed by men. Around half of patients routinely assumed alcohol (45.8%) and the 37.5% smoked. The main tumor site was the tongue (62.5%) with a preeminent moderate histological grade (66.6%). TNM stage was well distributed among the four categories. The main therapeutic approach was radiotherapy, while chemotherapy was used only in the 25% of patients. Only primary OSCC samples with histologically tumor-free CM were included in the study. Indeed, as shown in the representative images of hematoxylin and eosin staining, T showed neoplastic proliferation of pleomorphic cells, CM showed a mild dysplasia with atypical tissue morphology only at the inner epithelial layers, and DM showed a mild hyperplasia without any signs of disrupted tissue morphology (10x and 20x images in Fig 1A). First, Principal Component

Table 1. Demographic and clinicopathological characteristics of OSCC patients (n = 24).

VARIABLES			NUMBER (n)	PERCENTAGE (%)
Patient enrolled			24	
Age (years)	Mean (range)	68.6 (47 to 89)		
Sex	Male		14	58.3
	Female		10	41.6
Alcohol			11	45.8
Smoke			9	37.5
Site of tumor	Alveolar mucosa		6	25
	Tongue		15	62.5
	Cheek		3	12.5
Histologic grade	Well		5	20.8
	Moderate		16	66.6
	Poor		3	12.5
T stage	T1		14	58.3
	T2		4	16.6
	T3		5	20.8
	T4		1	4.1
N stage	N0		15	62.5
	N1		5	20.8
	N2		4	16.6
M stage	M0		24	100
	M1		0	0
TNM Stage	I		9	37.5
	II		3	12.5
	III		7	29.1
	IVA		5	20.8
Chemotherapy	No		18	75
	Yes		6	25
Radiotherapy	No		14	58.3
	Yes		10	41.6

https://doi.org/10.1371/journal.pone.0293475.t001

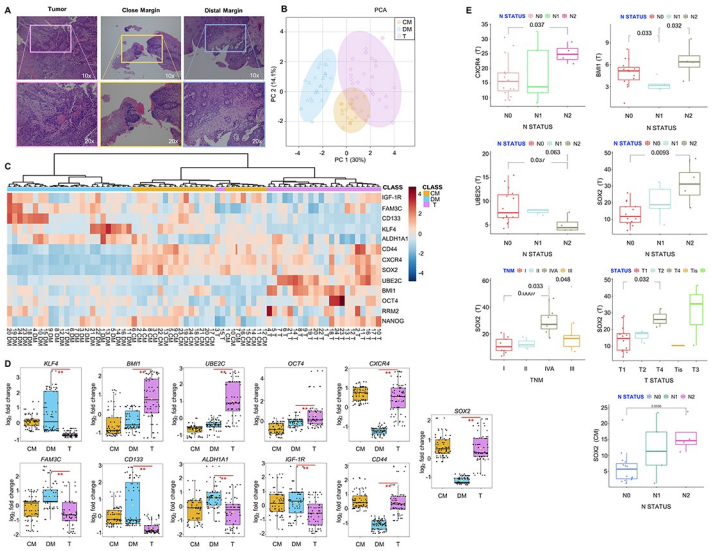

Fig 1. High *SOX2* in T and CM samples correlate with N status of patients with OSCC. (A) Representative images of tumor (T), close margin (CM), and distal margin (DM) tissue specimens stained with hematoxylin and eosin (10x and 20x magnification). **(B)** Principal component analysis (PCA), **(C)** unsupervised hierarchical clustering analysis, and **(D)** relative box plots showing gene expression pattern and levels (log_2 |FC|) in T, CM, and DM samples (T *vs* DM, ** *p*-value < 0.01; CM *vs* DM, ** *p*-value < 0.01). **(E)** Correlation between *CXCR4*, *BMI*, *UBE2C*, *SOX2* expression in T and CM with TNM stage, tumor size (T status), and lymph node metastasis (N status) (*p*-value < 0.05 is statistically significant).

https://doi.org/10.1371/journal.pone.0293475.g001

Analysis (PCA) and unsupervised hierarchical clustering analysis confirmed that, overall, T samples were consistently different from DM samples (Fig 1B and 1C). In detail, *SOX2*, *BMI1*, *UBE2C*, *OCT4*, *CXCR4*, and *CD44* were significantly upregulated in T *vs* DM (Log_2|FC| >1, ** *p*-value < 0.01) while *KLF4*, *FAM3C*, *ALDH1A1*, *CD133*, and *IGF-1R* were significantly downregulated in T *vs* DM (Log_2|FC| <1, ** *p*-value < 0.01) (Fig 1D). Then, we interestingly found that CM samples appeared partially clustering with T (Fig 1B and 1C). Indeed, for some patients, *SOX2*, *CXCR4*, and *CD44* expression levels in CM samples were similar to those observed in their relative T samples and higher than those observed in DM (Fig 1D). For *SOX2*, this trend was confirmed also at the protein level by Western Blot (WB) (see patient #2 in S1 Fig). No significant differences were observed in *NANOG* and *RRM2* (S2 Fig).

Analysis of clinicopathological correlations showed that high levels of *SOX2* in T significantly correlated with a higher TNM stage [32] (stage IVA vs stage I, *p*-value = 0.0007; stage IVA vs stage II, *p*-value = 0.033; stage IVA vs stage III, *p*-value = 0.048) while high levels of *CXCR4* and *BMI1* significantly correlated with a greater lymph node compromise (N status) (*CXCR4*: N2 vs N0, *p*-value = 0.037) (*BMI1*: N2 vs N1, *p*-value = 0.032). Patients with greater N status also showed significantly lower *UBE2C* levels in T (N2 vs N0, *p*-value = 0.037). Notably, high levels of *SOX2* in CM significantly correlated with lymph node compromise (N2 *vs* N0, log_2 |FC| = 1.32, *p*-value = 0.0036). Overall, these data suggest that SOX2 might be involved in OSCC local spreading.[NO_PRINTED_FORM]

TCGA analysis of CSCs markers in HNSCC

OSCC accounts for more than 90% of HNSCC [1,2]. Thus, we employed the RNA-seq data relative to 520 primary HNSCC tissue specimens and 44 healthy mucosa samples archived in TCGA to confirm the impact of the above mentioned 13 CSCs markers on patient outcomes.

We found that *BMI1*, *CD44*, *SOX2*, *OCT4*, *UBE2C*, *FAM3C*, *CXCR4*, *NANOG*, and *RRM2* mRNA levels were significantly increased while *IGF-1R*, *KLF4*, and *ALDH1A* were decreased in OSCC samples compared to healthy adjacent mucosa and that this trend significantly correlated with tumor stage (Fig 2). Patients harboring low/medium expression of *CXCR4* in tumor samples showed a worse overall survival (OS) (p-value = 0.0055). No significant impact on OS was observed for all the other DEGs (Fig 3).

SOX2 knockdown reduces OSCC cell migration ability

To investigate the contribution of SOX2 in the development of an aggressive and invasive OSCC phenotype, we performed its transient knockdown in CAL27 and SCC15 OSCC cell lines (Fig 4A). Then, we performed wound healing assays upon 24h, 48h and 72h transfection with siSOX2 and, as reported in representative images and relative histograms, we observed that *SOX2* knockdown reduced *in vitro* migration of both CAL27^{siSOX2} and SCC15^{siSOX2} (*p-value < 0.05, 72h CAL27) (*p-value < 0.05, 24h SCC15) (**p-value < 0.01, 48h SCC15) (**p-value < 0.01, 72h SCC15) (Fig 4B; S1–S4 Movies). Because tumor migration is tightly associated with epithelial-to-mesenchymal transition (EMT), we further measured the expression levels of key EMT markers vimentin (*VIM*) and e-cadherin (*E-CAD*) and mediators (*SNAIL* and *SLUG*). Interestingly, we found that *SOX2* knockdown strongly reduced both mRNA and protein expression of the mesenchymal marker *VIM* and that of the EMT-associated transcription factor *SNAIL* in both cell lines (*p-value <0.05) (Fig 4C). In agreement with *in vitro* data, we found that both in T and CM samples, higher levels of *SOX2* correlate with lower levels of *E-CAD* and higher levels of *VIM*, compared to T and CM samples showing low levels of *SOX2* (*p-value < 0.05) (S3A and S3B Fig). Finally, WB analyses showed that SOX2 knockdown was associated with the reduction of pAKT protein levels thus suggesting a repression of AKT signaling pathway (Fig 4D).

SOX2 knockdown attenuates CSCs-associated properties of OSCC cells

Next, we tested the effect of *SOX2* silencing on OSCC cell anchorage-independent growth by performing 3D tumor spheroid assay. As reported in representative images and relative

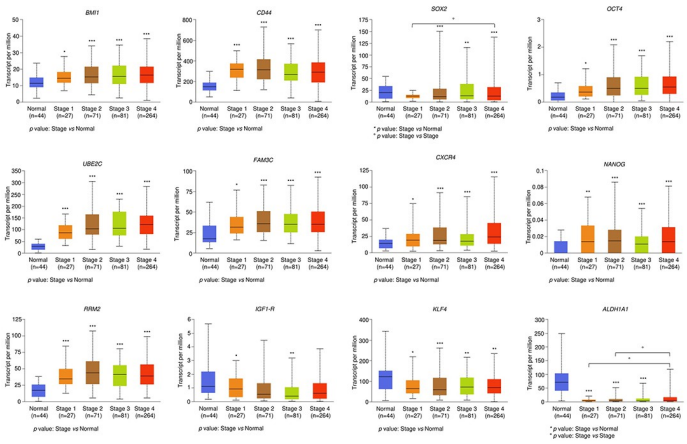

Fig 2. Correlation between CSCs markers and tumor stage in HNSCC patients. Correlation between the expression of CSCs markers and tumor stage in a cohort of primary HNSCC tissue specimens (n = 520) derived from TCGA dataset. CSCs expression markers are reported also in healthy mucosa samples (normal, n = 44). p-value Stage *vs* Normal: * < 0.05, ** < 0.01, *** < 0.001; p-value Stage *vs* Stage: ° < 0.05.

https://doi.org/10.1371/journal.pone.0293475.g002

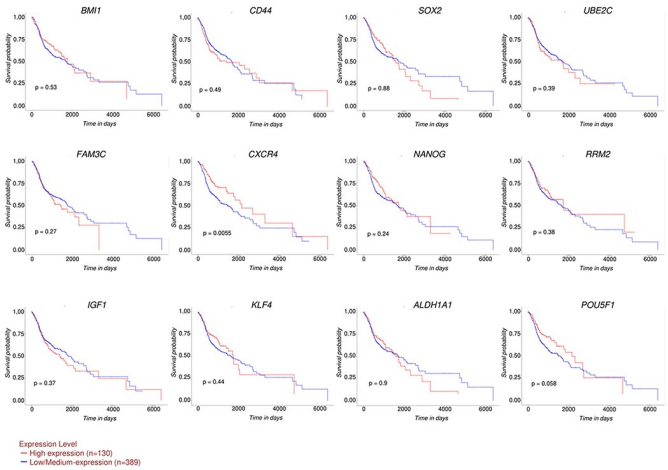

Fig 3. Impact of CSCs markers expression on overall survival (OS) of HNSCC patients. Kaplan-Maier OS curves of patients harboring high (n = 130, red line) and low/medium (n = 389, blue line) expression of CSCs markers. *p*-value < 0.05 was considered statistically significant.

https://doi.org/10.1371/journal.pone.0293475.g003

histograms, *SOX2* knockdown significantly reduced the number of tumor spheroids from a mean of 164.21 to 139.81 in CAL27 and from 200.15 to 147.65 in SCC15 cells (*p-value < 0.05, CAL27) (**p-value < 0.01, SCC15). Moreover, *SOX2* knockdown significantly also affected the spheroids diameter as demonstrated by the reduction from 193.66 μm to 134.39 μm in CAL27 and from 192.39 μm to 131.26 μm in SCC15 cells (*p-value < 0.05) (Fig 5A; S5–S8 Movies). In line with these results, we found that *SOX2* knockdown decreased the expression of a consistent number of other CSCs markers (*BMI1*, *UBE2C*, *CD44*, *NANOG*, *CXCR4*,

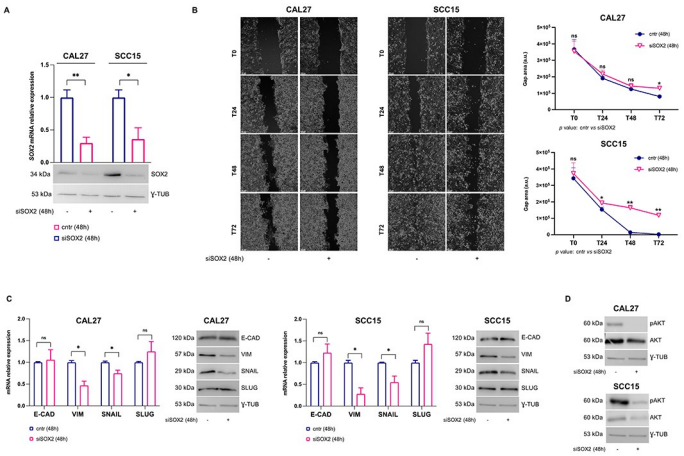

Fig 4. *SOX2* knockdown decreases OSCC cell migration and EMT. (A) qRT-PCR and western blot analyses of SOX2 in CAL27 and SCC15 cells (siSOX2 *vs* cntr). γ-TUB was used as a normalization control for protein quantification. **(B)** Representative images of wound healing assay of CAL27 and SCC15 cells (siSOX2 *vs* cntr) at T0, T24, T48, and T72 (10x magnification) (left); Mean and SD of the gap area (a.u.: arbitrary unit) of three biological replicates (right). **(C)** qRT-PCR and WB analysis of EMT markers in both cell lines upon *SOX2* knockdown. **(D)** WB analysis of pAKT/AKT in both cell lines upon *SOX2* knockdown. All the experiments were carried out in triplicate. qRT-PCR are presented as mean ± SD. *p*-value: *< 0.05, ** < 0.01. ns: not significant.

https://doi.org/10.1371/journal.pone.0293475.g004

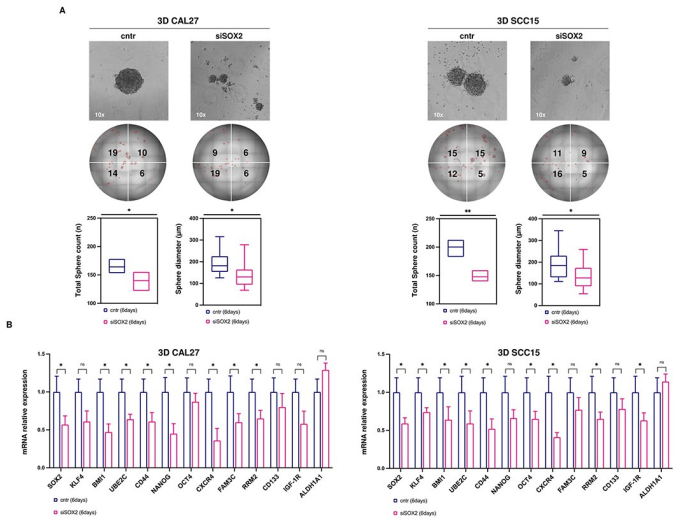

Fig 5. *SOX2* knockdown mitigates the stemness properties of OSCC cells. (A) Representative images and relative histograms of 3D tumor spheroid morphology, count, and diameter in CAL27 and SCC15 cells (siSOX2 *vs* cntr). **(B)** qRT-PCR analysis of a panel of stemness genes in both cell lines upon *SOX2* knockdown. All the experiments were carried out in triplicate and results are presented as mean ± SD. *p*-value: *< 0.05, ** < 0.01. ns: not significant.

https://doi.org/10.1371/journal.pone.0293475.g005

FAM3C, and *RRM2*) in both CAL27 and SCC15 3D tumor spheroids (*p-value <0.05) (Fig 5B).

Targeting *SOX2* improves sensitivity to cisplatin treatment in OSCC cells

The observation that *SOX2* supports oral squamous CSCs properties was suggestive of its possible involvement in the modulation of response of OSCC to chemotherapy. Thus, we treated CAL27^{siSOX2} and SCC15^{siSOX2} cells and relative control cells with growing concentration of cisplatin (6μM, 12μM, 24μM, 48μM) for 24h upon 48h transient transfection with siSOX2 and negative control siRNA, respectively. As shown in Fig 6A and 6B, *SOX2* knockdown significantly improved sensitivity of CAL27 cells at 12μM, 24μM and 48μM of cisplatin (*p-value <0.05 12μM and 24μM) (**p-value <0.01 48μM) by increasing the percentage of cells undergoing apoptosis compared to control cells. This effect was confirmed in SCC15 cells only upon treatment with 24μM cisplatin (*p-value <0.05).

Discussion

It is well known that the OSCC core is populated by a small fraction of CSCs, which may represent the culprits behind the anchorage-independent growth, migration, and spreading of tumor cells [33]. The presence within the OSCC margins of a subpopulation of CSCs that may function as cancer-initiating cells and, thus. may massively contribute to local recurrence, still remains obscure because of the lack of surrogate biomarkers.

In the present study, whose experimental workflow is schematically reported in Fig 7, we demonstrate that the OSCC is defined by a CSCs-associated molecular signature characterized by high levels of *SOX2*, *BMI1*, *UBE2C*, *OCT4*, *CXCR4*, and *CD44* and low levels of *CD133*, *KLF4*, *ALDH1A1*, and *IGF-1R*. Notably, high levels of *SOX2*, *BMI1*, and *CXCR4*, as well as low levels of *UBE2C* in the tumor core (T) significantly correlate with a greater tumor size and lymph node compromise. Due to the short follow-up period (<3 years), our cohort of patients did not show distant metastasis (M status) or death events, so correlations with M status or OS

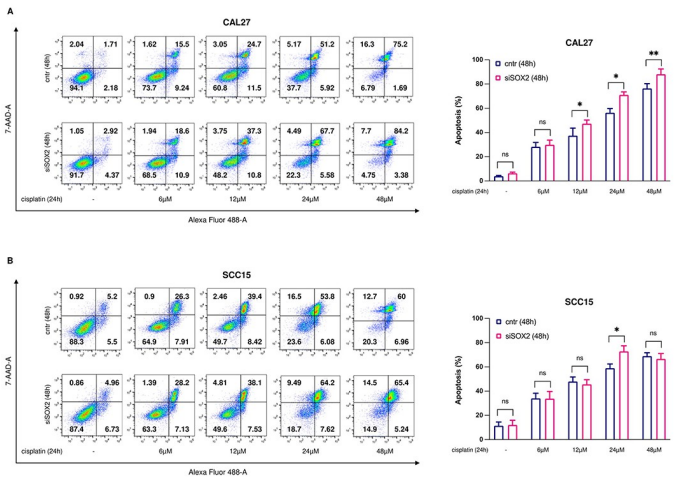

Fig 6. *SOX2* silencing increases apoptosis in OSCC cells upon cisplatin administration. (A-B) Representative plots of Annexin V/7-AAD apoptosis assay (left) in CAL27 and SCC15 cells (siSOX2 *vs* cntr) upon treatment with 6, 12, 24 and 48μM cisplatin (24h) and relative graphical data of total apoptotic cells (%) (right). All the experiments were carried out in triplicate and results are presented as mean ± SD. *p*-value: $^{*}< 0.05$, $^{**} < 0.01$. ns: not significant.

https://doi.org/10.1371/journal.pone.0293475.g006

were not available. These results were supported by TCGA analysis showing that the identified CSCs gene signature significantly correlates with advanced tumor stage, but not with OS, also in patients with HNSCC. [24,27,28,33–41]. The only exception was for *CXCR4*, whose high expression in HNSCC samples appears to correlate with a better OS.

The main finding of our study is that the close margin, defined as tumor-free by the conventional histopathological examination, may show high levels of *SOX2*, *CD44*, and *CXCR4* to an extent comparable to that observed in the relative tumor core. Most importantly, the high expression of *SOX2* in the close margin significantly correlates with a greater lymph node compromise, thus suggesting a possible role of this marker in fostering the progression of OSCC. Our results add an important piece of information to the current literature that, although

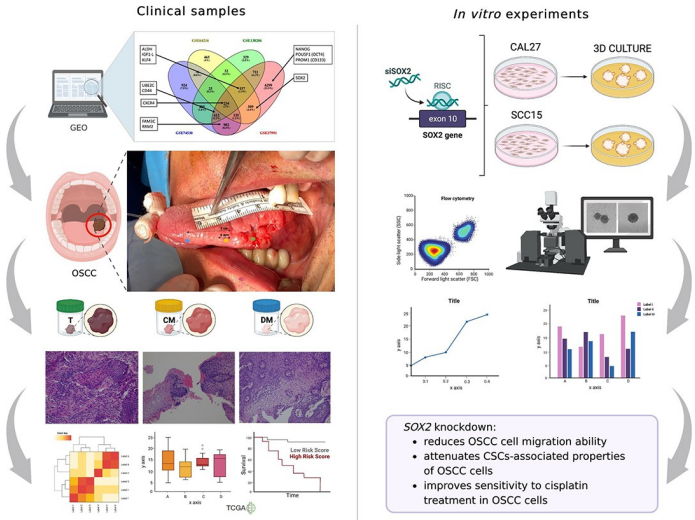

Fig 7. Schematic representation of the investigation workflow.

https://doi.org/10.1371/journal.pone.0293475.g007

seems to agree on the overexpression of SOX2 along the different steps of oral cancer [30], still remains debated on the role of SOX2 in OSCC progression [29,31,30] SOX2 has been correlated either to a favorable or an unfavorable prognosis. In support of a role as favorable prognostic biomarker, it has been reported that *SOX2* is overexpressed during the early stages of OSCC and that this predicts for reduced local recurrence [42]. On the contrary, other studies have demonstrated that SOX2 overexpression promotes EMT and lymph node metastasis [42–47] while SOX2 knockdown inhibits HNSCC cell self-renewal and chemoresistance [34]. A recent retrospective study also highlights that *SOX2* is overexpressed in pre-malignant oral disorders and that this predicts for oral cancer evolution [42, 48].

A survey of the literature indicates that SOX2 affects tumor progression by acting on several signaling pathways in a context-dependent manner. SOX2 may promote EMT by transcriptionally activating SNAIL, SLUG, and TWIST, which in turn act as transcription factors involved in the repression of the epithelial marker E-CADHERIN and the activation of the mesenchymal marker VIMENTIN. In breast and pancreatic cancer, indeed, the overexpression of SOX2 leads to the EMT through the repression of the epithelial genes *E-CAD* and *Zo-1* [49,50]. SOX2 may promote the remodeling of the extracellular matrix (ECM). In lung cancer, indeed, SOX2 activates AKT/mTOR signaling pathway, which in turn enhances the activity of the matrix-metalloproteinase-2 (MMP2) [51]. [49–51] In prostate cancer, SOX2 fosters the EMT by directly binding to the β-catenin enhancer and thus activating the Wnt/β-catenin pathway [52]. In this regard, in this study we show that *SOX2* knockdown remarkably reduces the OSCC cells migration ability and that is associated with inhibition of the EMT as suggested by the significant reduction of SNAIL and VIMENTIN and the slight increase of E-CADHERIN. Furthermore, we show that *SOX2* silencing is associated with the repression of AKT signaling pathway as demonstrated by the reduction of pAKT protein levels.

In bladder cancer, tumor progression is associated with the strong up-regulation of SOX2 and NANOG and the consequent acquisition of cancer stem cell properties [53,54]. According to our results, silencing *SOX2* leads to the inhibition of anchorage-independent growth of CAL27 and SCC15 cells and, thus, to the significant reduction of 3D oral tumor spheroids generation.

A previous study highlighted that, in HNSCC, SOX2 triggers cisplatin resistance by promoting drug efflux via activation of the ATP-binding cassette ABCG22 (ABCG2) transporter [55]. In ovarian cancer SOX2 ectopic overexpression promotes tumor cell resistance to several chemotherapeutic compounds, such as cisplatin, carboplatin, and paclitaxel, by altering the homeostasis between pro- and anti-apoptotic proteins. Conversely, *SOX2* knockdown restores drug sensitivity by causing mitochondrial dysfunction, apoptosis, and autophagy [56]. In EGFR-mutated lung cancer cells, *SOX2* overexpression promotes resistance to erlotinib by repressing the expression of proapoptotic proteins BIM and BMF [57]. Concerning the role of SOX2 in OSCC response to chemotherapy, our results indicate that the loss of *SOX2* improves CAL27 and SCC15 sensitivity to cisplatin treatment by increasing the percentage of apoptotic events. However, further detailed mechanisms underlying the contribution of *SOX2* to a more aggressive behavior remain to be entirely elucidated and will be subject of future studies.

Collectively, our study underlines that the molecular analysis highlights the existence of residual tumor cells over-expressing CSCs markers even in the OSCC close margins defined as tumor-free by the conventional histopathological examination. In particular, we show for the first time that *SOX2* is over-expressed not only in the tumor core but also in the close margin of OSCC patients with advanced tumor stage and lymph node compromise, thus suggesting that high levels of *SOX2* may predict for a local spreading. Furthermore, we demonstrate that *SOX2* knockdown abrogates *in vitro* OSCC cell migration ability and CSCs-traits, and at the same time, improves OSCC cell sensitivity to cisplatin. Future *in vitro* and *in vivo* studies are

mandatory to investigate the molecular mechanisms underlying the role of *SOX2* in OSCC spreading and its potential as therapeutic target to prevent OSCC dissemination.

Materials and methods

In silico analysis through Gene Expression Omnibus (GEO database)

CSCs markers genes expression were explored using GEO database. Research queries included "Homo sapiens" and "oral squamous cell carcinoma" as keywords. After a survey of the literature, 4 datasets containing CSCs gene expression profiles of both OSCC, and healthy oral tissues were selected (S1 Table) and analyzed in R Software (Version: 1.3.1093) by using "limma" bioconductor package to identify the differentially expressed genes (DEGs) between OSCC and healthy tumor tissues. DEGs were selected by using the following criteria:$\log_2|FC| \geq 1$ and adjust p-value ≤ 0.05.

Patients and clinical samples

Twenty-four OSCC patients were surgically treated at the Oral Pathology and Oral Surgery Unit of "Magna Graecia" University, between December 2020 and December 2022. For each patient, primary tissue specimens were collected at 2 cm from the macroscopic lesion boundaries defined visually and by palpation. Laser Capture Microdissection (LCM) was used to obtain three different area from each biopsy: i) tumor core (T), ii) tumor-free close margin (CM) within 1–4.9 mm from the lesion boundaries and iii) adjacent health distant margin (DM) collected > 1.5 cm from the lesion boundaries, as recommended from current clinical guidelines [7,10,58,59]. Two μm serial sections were obtained from formalin-fixed and paraffin-embedded T, CM and DM tissue specimens. Samples collection was performed in the same two-year's time frame.

All patients provided a written informed consent at the time of data collection.

No information that could identify individual participants are available. The procedures reported in this study were performed in accordance with the Helsinki Declaration guidelines (2008) on human experimentation and good clinical practice (good clinical practice or GCP).

TCGA data analysis

A total of 564 samples were analyzed by TCGA Biolinks R Bioconductor [60] for the expression of 13 selected CSCs marker genes. OSCC samples were selected using ALCAN database, (http://ualcan.path.uab.edu/cgi-bin/ualcan-res.pl) [61].

Cell lines and culture

OSCC cell lines CRL-2095 (CAL27) and CRL-1623 (SCC15) derived from tongue squamous carcinoma were purchased from the American Type Culture Collection (ATCC, Rockville, MD, USA). CAL27 cells were grown in Dulbecco's Modified Eagle's Medium (DMEM) (Sigma-Aldrich, St. Louis, MO, USA) supplemented with 10% (v/v) Fetal Bovine Serum (FBS) (Invitrogen, San Diego, CA, USA), and 1% (v/v) of penicillin and streptomycin 100 U/ml (Sigma-Aldrich, St. Louis, MO, USA). Conversely, for SCC15 cell line a 1:1 mixture of DMEM medium (Sigma-Aldrich, St. Louis, MO, USA) and Ham's F-12 Nutrient Mix (Thermo Fisher Scientific, Waltham, MA, USA), supplemented with 90% (v/v) hydrocortisone 400 ng/ml (Sigma-Aldrich, St. Louis, MO, USA), 10% FBS, and 1% (v/v) of penicillin/streptomycin 100 U/ml was used. Cells were maintained in a 5% CO_2 humidified atmosphere at 37˚C and routinely examined for Mycoplasma contamination. CAL27 and SCC15 were selected for their ability to generate three-dimensional (3D) tumor spheroid *in vitro*.

RNA isolation, cDNA generation, and Real-time quantitative reverse transcription (qRT)-PCR

Total RNA was isolated using TRIzol™ Reagent (Life Technologies, Carlsbad, CA, USA) according to the manufacturer's instructions. Extracted RNA quality and quantification were assessed using NanoDrop® ND-1000 (Thermo Fisher Scientific, Waltham, MA, USA) [62–64]. Then, 1μg of total RNA were retrotranscribed using High-Capacity cDNA Reverse Transcription Kit (Thermo Fisher Scientific, Waltham, Massachusetts, USA). Synthesized cDNA (50 ng) was used for qRT-PCR performed using SYBR™ Green PCR Master Mix (Thermo Fisher Scientific, Waltham, Massachusetts, USA), and 400 nM of each primer pair [65]. Genes analyzed were as follow: *E-CAD*, *VIM*, *SNAIL*, *SLUG*, *SOX2*, *KLF4*, *BMI1*, *UBE2C*, *CD44*, *NANOG*, *OCT4*, *CXCR4*, *FAM3C*, *RRM2*, *CD133*, *IGF-1R*, and *ALDH1A1*. The thermal profile used were structured as follow: 1 step at 95˚C for 10 min, 45 cycles at 95˚C for 30 sec, and 60 sec at 60˚C. The relative mRNA expression level was calculated by the $2^{-\Delta\Delta Ct}$ method using *GAPDH* or *RPL38* as housekeeping genes for cell lines or tissue specimens, respectively [66]. Each reaction was performed in triplicate.

Western blot

Protein extraction and Western Blot were performed as previously reported by Chirillo R et al [67]. Antibodies against SOX2 (1:500, sc-365823), VIM (1:500, sc-7557), E-CAD (1:500, sc-8426), SLUG (1:500, sc-166476), SNAIL (1:500, sc-393172) were purchased from Santa Cruz Biotechnology (Santa Cruz Biotechnology, Dallas, Texas, USA); antibodies against AKT (1:1000, #9272) and p-AKT (1:1000, #9271) were obtained from Cell Signaling Technology (Danvers, Massachusetts, USA). Goat polyclonal anti-γ-Tubulin antibody (1:3000; sc-7396) (Santa Cruz Biotechnology, Dallas, TX, USA) and RPL38 (1:1000, PA5-88313) (Thermo Fisher, Waltham, MA, USA) served as a reference for samples loading. The membranes were washed for 30 min with T-TBS solution and then incubated for 1h at room temperature with peroxidase-conjugated secondary antibodies (Peroxidase AffiniPure Sheep Anti-Mouse IgG, 1:10000; Peroxidase AffiniPure Donkey Anti-Goat IgG, 1:10000) (Jackson ImmunoResearch Labs, West Grove, PA, USA). Chemiluminescence signals were detected using Western Blotting Luminol Reagent (Santa Cruz Biotechnology, Dallas, TX, USA) and acquired by UVItec Alliance Mini HD9 (UVItec Ltd. Cambridge, Cambridge, UK). The protein band intensity on western blots was quantified and normalized using ImageJ Software (http://rsb.info.nih.gov/ij/) [68–70].

SOX2 transient knockdown

CAL27 and SCC15 cells were transfected using Lipofectamine™ 3000 Transfection Reagent (Thermo Fisher Scientific, Waltham, MA, USA) according to the manufacturer's protocol. SOX2 siRNA was purchased from Thermo Fisher Scientific. To ensure an optimal control, the two cell lines were further transfected with Silencer™ Select Negative Control siRNA (cntr) (Thermo Fisher Scientific, Waltham, MA, USA). The evaluation of transfection efficiency was performed by western blot and qRT-PCR at 48h [71].

Wound healing assay

$1x10^6$ cells/well were seeded in 6-wells standard plates. To simulate a wound, the cells monolayer was manually scratched using a pipette tip. Wound closure was then monitored through images and time-lapse video recorded at 0, 24 and 48h using Leica THUNDER Imaging

Systems DMi8 (Leica Microsystems S.r.l., Wetzlar, Germany). Subsequently, cell migration was quantified by Leica Application Suite Software [72].

3D tumor spheroid assay

CAL27 and SCC15 were seeded in Corning® Costar® Ultra-Low Attachment Multiple Well Plates (Corning Inc., New York, NYC, USA) at a concentration of $15x10^3$ cells/mL. OSCC 3D tumor spheroids were cultured in a previously described sphere medium [73]. OSCC tumor spheroids were grown in a 5% CO_2 humidified atmosphere at 37˚C and monitored through images and time-lapse video recorded for 6 days using Leica THUNDER Imaging Systems DMi8 (Leica Microsystems S.r.l., Wetzlar, Germany). The collected tumor spheroids were resuspended in an appropriate volume of culture medium and counted according to the following formulas:

$$sphere\ concentration = sphere\ count \div counting\ volume\ (\mu L)$$

$$total\ sphere\ count = sphere\ concentration \times total\ volume$$

Their diameters were then measured through the internal image measuring feature of Leica Application Suite Software.

Cisplatin treatment

$CAL27^{cntr}$, $CAL27^{siSOX2}$, $SCC15^{cntr}$, $SCC15^{siSOX2}$ were seeded in 6-wells standard plates. Cisplatin was added into the medium at various concentrations (6μM, 12μM, 24μM, 48μM) for 24h. Treatment was performed upon 48h of transient transfection with siSOX2 or negative control siRNA, respectively.

Flow cytometry apoptosis analysis

To identify cells actively undergoing apoptosis, a double staining with Annexin V and PI was performed using Alexa Fluor®488 Annexin V/Dead Cell Apoptosis Kit (Thermo Fisher Scientific, Waltham, MA, USA) according to the manufacturer's instructions. Cells were then incubated at room temperature for 15 min in the dark. Each tube was diluted with 400μL of Annexin Binding Buffer. Flow cytometry assays were performed using the BD LSRFortessa™ X-20 (BD Biosciences, San Jose, CA, USA). Data analysis was carried out using FlowJo™ v10 Software (BD Biosciences, San Jose, CA) [72,74,75].

Statistical analysis

Statistical tests were conducted using GraphPad Prism 9 and R software. Gene expression data were analyzed by Principal Component Analyisis (PCA) and unsupervised hierarchical clustering. ANOVA multi-sample test (permutation-based 5% FDR) was performed on the resulting dataset, and the significant DEGs were grouped by unsupervised hierarchical clustering. Multivariate correlations between gene expression data and clinicopathological parameters were performed using a Cox's multiple linear regression model based on Firth's bias correction method. The statistical significance of the *in vitro* experimental data was analyzed using the two-tailed Student's t-test (for comparisons of two treatment groups) or one-way ANOVA (for comparisons of three or more groups). All results were expressed as the means ± standard deviation (SD). A p-value ≤ 0.05 was considered statistically significant.

Supporting information

S1 Fig. SOX2 protein levels in T, CM, and DM of two representative OSCC samples. WB analysis of SOX2 in T, CM, and DM samples of two representative OSCC patients (#1 and #2) and relative optical densitometry. In patient #1, SOX2 protein level is higher in T compared to CM and DM. In patient #2, SOX2 protein level is similar in T and CM and higher compared to DM. RPL38 was used as a normalization control for protein quantification.
(PDF)

S2 Fig. *NANOG* and *RRM2* did not show any significant difference among T, CM and DM samples. Box plots showing *NANOG* and *RRM2* gene expression levels ($\log_2$ |FC|) in T, CM, and DM samples (ns: not significant).
(PDF)

S3 Fig. High *SOX2* levels correlate with EMT phenotype in tissue samples. Box plots showing the relative expression of *VIM* and *E-CAD* in both T **(A)** and CM **(B)** samples clustered according to high or low *SOX2* levels, respectively (*ANOVA t-test p value < 0.05).
(PDF)

S1 Table. Details of the selected four databases.
(PDF)

S1 Raw images. Uncropped plots relative to all Western Blot analyses. (A) Uncropped plot relative to Western Blot analysis (showed in Fig 4A) of SOX2 in CAL27 and SCC15 cells (siSOX2 *vs* cntr). γ-TUB was used as a normalization control for protein quantification. **(B-C)** Uncropped plot relative to Western Blot analyses (showed in Fig 4C) of EMT markers (E-CAD, VIM, SLUG, SNAIL) in CAL27 and SCC15 cells (siSOX2 *vs* cntr). γ-TUB was used as a normalization control for protein quantification. **(D)** Uncropped plot relative to Western Blot analyses (showed in Fig 4D) of AKT and p-AKT in CAL27 and SCC15 cells (siSOX2 *vs* cntr). γ-TUB was used as a normalization control for protein quantification. **(E)** Uncropped blot relative to Western Blot analysis (showed in S1 Fig) of SOX2 in T, CM and DM samples of two representative patients (#1 and #2). RPL38 was used as a normalization control for protein quantification.
(DOCX)

S1 Movie. Time lapse of wound healing assay of CAL27 cntr for 72h (10x magnification).
(MP4)

S2 Movie. Time lapse of wound healing assay of CAL27 siSOX2 for 72h (10x magnification).
(MP4)

S3 Movie. Time lapse of wound healing assay of SCC15 cntr for 72h (10x magnification).
(MP4)

S4 Movie. Time lapse of wound healing assay of SCC15 siSOX2 for 72h (10x magnification).
(MP4)

S5 Movie. Time lapse of 3D tumor spheroid formation assay of CAL27 cntr for 6 days (10x magnification).
(MP4)

S6 Movie. Time lapse of 3D tumor spheroid formation assay of CAL27 siSOX2 for 6 days (10x magnification).
(MP4)

S7 Movie. Time lapse of 3D tumor spheroid formation assay of SCC15 cntr for 6 days (10x magnification).
(MP4)

S8 Movie. Time lapse of 3D tumor spheroid formation assay of SCC15 siSOX2 for 6 days (10x magnification).
(MP4)

Acknowledgments

We thank the Center of Interdepartmental Services (CIS), "Magna Graecia" University of Catanzaro for the experimental support.

Author Contributions

Conceptualization: Flavia Biamonte, Amerigo Giudice.

Data curation: Alessandro Sacco, Anna Martina Battaglia, Gianluca Santamaria, Ilenia Aversa, Flavia Biamonte, Amerigo Giudice.

Formal analysis: Alessandro Sacco, Anna Martina Battaglia, Gianluca Santamaria, Anna Procopio, Anna Maria Lavecchia, Ilenia Aversa.

Investigation: Alessandro Sacco, Anna Martina Battaglia, Ilenia Aversa, Emanuele Giorgio, Lavinia Petriaggi, Flavia Biamonte, Amerigo Giudice.

Methodology: Alessandro Sacco, Anna Martina Battaglia, Gianluca Santamaria, Caterina Buffone, Selene Barone, Anna Procopio, Anna Maria Lavecchia, Ilenia Aversa, Maria Giulia Cristofaro.

Project administration: Anna Martina Battaglia, Flavia Biamonte, Amerigo Giudice.

Resources: Caterina Buffone, Selene Barone, Anna Maria Lavecchia, Maria Giulia Cristofaro, Flavia Biamonte, Amerigo Giudice.

Software: Gianluca Santamaria, Anna Procopio.

Supervision: Flavia Biamonte, Amerigo Giudice.

Validation: Alessandro Sacco, Anna Martina Battaglia, Ilenia Aversa, Flavia Biamonte, Amerigo Giudice.

Visualization: Alessandro Sacco, Anna Martina Battaglia, Gianluca Santamaria, Flavia Biamonte, Amerigo Giudice.

Writing – original draft: Alessandro Sacco, Anna Martina Battaglia, Flavia Biamonte, Amerigo Giudice.

References

1. Vigneswaran N, Williams MD. Epidemiologic trends in head and neck cancer and aids in diagnosis. Oral Maxillofac Surg Clin North Am. 2014; 26: 123–141. https://doi.org/10.1016/j.coms.2014.01.001 PMID: 24794262

2. Farooq I, Bugshan A. Oral squamous cell carcinoma: metastasis, potentially associated malignant disorders, etiology and recent advancements in diagnosis. F1000Res. 2020; 9. https://doi.org/10.12688/f1000research.22941.1 PMID: 32399208
3. Huang SH, O'Sullivan B. Oral cancer: Current role of radiotherapy and chemotherapy. Med Oral Patol Oral Cir Bucal. 2013; 18: e233. https://doi.org/10.4317/medoral.18772 PMID: 23385513
4. Liu Y, Yang M, Luo J, Zhou H. Radiotherapy targeting cancer stem cells "awakens" them to induce tumour relapse and metastasis in oral cancer. International Journal of Oral Science 2020 12:1. 2020; 12: 1–12. https://doi.org/10.1038/s41368-020-00087-0 PMID: 32576817
5. Li Q, Liu X, Wang D, Wang Y, Lu H, Wen S, et al. Prognostic value of tertiary lymphoid structure and tumour infiltrating lymphocytes in oral squamous cell carcinoma. International Journal of Oral Science 2020 12:1. 2020; 12: 1–8. https://doi.org/10.1038/s41368-020-00092-3 PMID: 32934197
6. Suganya AAS, Kochurani KJ, Nair MG, Louis JM, Sankaran S, Rajagopal R, et al. TM1-IR680 peptide for assessment of surgical margin and lymph node metastasis in murine orthotopic model of oral cancer. Scientific Reports 2016 6:1. 2016; 6: 1–9. https://doi.org/10.1038/srep36726 PMID: 27827443
7. Nason RW, Binahmed A, Pathak KA, Abdoh AA, Sándor GKB. What is the adequate margin of surgical resection in oral cancer? Oral Surgery, Oral Medicine, Oral Pathology, Oral Radiology, and Endodontology. 2009; 107: 625–629. https://doi.org/10.1016/j.tripleo.2008.11.013 PMID: 19168372
8. Minhas S, Kashif M, Altaf W, Afzal N, Nagi AH. Concomitant-chemoradiotherapy-associated oral lesions in patients with oral squamous-cell carcinoma. Cancer Biol Med. 2017; 14: 176. https://doi.org/10.20892/j.issn.2095-3941.2016.0096 PMID: 28607808
9. van Lanschot CGF, Mast H, Hardillo JA, Monserez D, ten Hove I, Barroso EM, et al. Relocation of inadequate resection margins in the wound bed during oral cavity oncological surgery: A feasibility study. Head Neck. 2019; 41: 2159–2166. https://doi.org/10.1002/hed.25690 PMID: 30706624
10. Dillon JK, Brown CB, McDonald TM, Ludwig DC, Clark PJ, Leroux BG, et al. How Does the Close Surgical Margin Impact Recurrence and Survival When Treating Oral Squamous Cell Carcinoma? Journal of Oral and Maxillofacial Surgery. 2015; 73: 1182–1188. https://doi.org/10.1016/j.joms.2014.12.014 PMID: 25795179
11. Biamonte F, Buffone C, Santamaria G, Battaglia AM, Mignogna C, Fortunato L, et al. Gene expression analysis of autofluorescence margins in leukoplakia and oral carcinoma: A pilot study. Oral Dis. 2021; 27: 193–203. https://doi.org/10.1111/odi.13525 PMID: 32645756
12. Machiels J-P, René Leemans C, Golusinski W, Grau C, Licitra L, Gregoire V, et al. Reprint of "Squamous cell carcinoma of the oral cavity, larynx, oropharynx and hypopharynx: EHNS-ESMO-ESTRO Clinical Practice Guidelines for diagnosis, treatment and follow-up". Oral Oncol. 2021; 113: 105042. https://doi.org/10.1016/j.oraloncology.2020.105042 PMID: 33583513
13. van Nieuwenhuizen AJ, Buffart LM, Langendijk JA, Vergeer MR, Voortman J, Leemans CR, et al. Health-related quality of life and overall survival: a prospective study in patients with head and neck cancer treated with radiotherapy. Qual Life Res. 2021; 30: 1145–1153. https://doi.org/10.1007/s11136-020-02716-x PMID: 33289866
14. Rohde M, Rosenberg T, Pareek M, Nankivell P, Sharma N, Mehanna H, et al. Definition of locally recurrent head and neck squamous cell carcinoma: a systematic review and proposal for the Odense-Birmingham definition. Eur Arch Otorhinolaryngol. 2020; 277: 1593–1599. https://doi.org/10.1007/s00405-020-05953-5 PMID: 32266461
15. Farah CS, McIntosh L, Georgiou A, McCullough MJ. Efficacy of tissue autofluorescence imaging (velscope) in the visualization of oral mucosal lesions. Head Neck. 2012; 34: 856–862. https://doi.org/10.1002/hed.21834 PMID: 21818819
16. Farah CS, Kordbacheh F, John K, Bennett N, Fox SA. Molecular classification of autofluorescence excision margins in oral potentially malignant disorders. Oral Dis. 2018; 24: 732–740. https://doi.org/10.1111/odi.12818 PMID: 29243374
17. Evans M, Beasley M. Target delineation for postoperative treatment of head and neck cancer. Oral Oncol. 2018; 86: 288–295. https://doi.org/10.1016/j.oraloncology.2018.08.011 PMID: 30409314
18. Thomas Robbins K, Triantafyllou A, Suárez C, López F, Hunt JL, Strojan P, et al. Surgical margins in head and neck cancer: Intra- and postoperative considerations. Auris Nasus Larynx. 2019; 46: 10–17. https://doi.org/10.1016/j.anl.2018.08.011 PMID: 30172560
19. Braakhuis BJM, Leemans CR, Brakenhoff RH. A genetic progression model of oral cancer: Current evidence and clinical implications. Journal of Oral Pathology and Medicine. 2004; 33: 317–322. https://doi.org/10.1111/j.1600-0714.2004.00225.x PMID: 15200478
20. Kujan O, Khattab A, Oliver RJ, Roberts SA, Thakker N, Sloan P. Why oral histopathology suffers inter-observer variability on grading oral epithelial dysplasia: an attempt to understand the sources of variation. Oral Oncol. 2007; 43: 224–231. https://doi.org/10.1016/j.oraloncology.2006.03.009 PMID: 16931119

21. Vicky De Boer D, Brink A, Buijze M, van Walsum MS, Hunter KD, Ylstra B, et al. Establishment and Genetic Landscape of Precancer Cell Model Systems from the Head and Neck Mucosal Lining. Mol Cancer Res. 2019; 17: 120–130. https://doi.org/10.1158/1541-7786.MCR-18-0445 PMID: 30224542

22. van Zeeburg HJT, Graveland AP, Brink A, Nguyen M, Leemans CR, Bloemena E, et al. Generation of precursor cell lines from preneoplastic fields surrounding head and neck cancers. Head Neck. 2013; 35: 568–574. https://doi.org/10.1002/hed.23004 PMID: 22714984

23. Pierik AS, Leemans CR, Brakenhoff RH. Resection Margins in Head and Neck Cancer Surgery: An Update of Residual Disease and Field Cancerization. Cancers (Basel). 2021; 13. https://doi.org/10.3390/cancers13112635 PMID: 34071997

24. Simple M, Suresh A, Das D, Kuriakose MA. Cancer stem cells and field cancerization of Oral squamous cell carcinoma. Oral Oncol. 2015; 51: 643–651. https://doi.org/10.1016/j.oraloncology.2015.04.006 PMID: 25920765

25. Baniebrahimi G, Mir F, Khanmohammadi R. Cancer stem cells and oral cancer: insights into molecular mechanisms and therapeutic approaches. Cancer Cell International 2020 20:1. 2020; 20: 1–15. https://doi.org/10.1186/s12935-020-01192-0 PMID: 32280305

26. Richard V, Kumar TRS, Pillai RM. Transitional dynamics of cancer stem cells in invasion and metastasis. Transl Oncol. 2021; 14: 100909. https://doi.org/10.1016/j.tranon.2020.100909 PMID: 33049522

27. Thankamony AP, Saxena K, Murali R, Jolly MK, Nair R. Cancer Stem Cell Plasticity–A Deadly Deal. Front Mol Biosci. 2020; 7: 79. https://doi.org/10.3389/fmolb.2020.00079 PMID: 32426371

28. Koo BS, Lee SH, Kim JM, Huang S, Kim SH, Rho YS, et al. Oct4 is a critical regulator of stemness in head and neck squamous carcinoma cells. Oncogene 2015 34:18. 2014; 34: 2317–2324. https://doi.org/10.1038/onc.2014.174 PMID: 24954502

29. Fu TY, Hsieh IC, Cheng JT, Tsai MH, Hou YY, Lee JH, et al. Association of OCT4, SOX2, and NANOG expression with oral squamous cell carcinoma progression. Journal of Oral Pathology & Medicine. 2016; 45: 89–95. https://doi.org/10.1111/jop.12335 PMID: 26211876

30. Luiz ST, Modolo F, Mozzer I, dos Santos EC, Nagashima S, Camargo Martins AP, et al. Immunoexpression of SOX-2 in oral leukoplakia. Oral Dis. 2018; 24: 1449–1457. https://doi.org/10.1111/odi.12922 PMID: 29938872

31. Novak D, Hüser L, Elton JJ, Umansky V, Altevogt P, Utikal J. SOX2 in development and cancer biology. Semin Cancer Biol. 2020; 67: 74–82. https://doi.org/10.1016/j.semcancer.2019.08.007 PMID: 31412296

32. Kato MG, Baek CH, Chaturvedi P, Gallagher R, Kowalski LP, Leemans CR, et al. Update on oral and oropharyngeal cancer staging–International perspectives. World J Otorhinolaryngol Head Neck Surg. 2020; 6: 66. https://doi.org/10.1016/j.wjorl.2019.06.001 PMID: 32426706

33. Al-Magsoosi MJN, Lambert DW, Ali Khurram S, Whawell SA. Oral cancer stem cells drive tumourigenesis through activation of stromal fibroblasts. Oral Dis. 2021; 27: 1383–1393. https://doi.org/10.1111/odi.13513 PMID: 32593227

34. Lee SH, Oh SY, Do SI, Lee HJ, Kang HJ, Rho YS, et al. SOX2 regulates self-renewal and tumorigenicity of stem-like cells of head and neck squamous cell carcinoma. Br J Cancer. 2014; 111: 2122. https://doi.org/10.1038/bjc.2014.528 PMID: 25321191

35. Huang C, Yoon C, Zhou XH, Zhou YC, Zhou WW, Liu H, et al. ERK1/2-Nanog signaling pathway enhances CD44(+) cancer stem-like cell phenotypes and epithelial-to-mesenchymal transition in head and neck squamous cell carcinomas. Cell Death & Disease 2020 11:4. 2020; 11: 1–14. https://doi.org/10.1038/s41419-020-2448-6 PMID: 32327629

36. Clarke MF, Dick JE, Dirks PB, Eaves CJ, Jamieson CHM, Jones DL, et al. Cancer stem cells—perspectives on current status and future directions: AACR Workshop on cancer stem cells. Cancer Res. 2006; 66: 9339–9344. https://doi.org/10.1158/0008-5472.CAN-06-3126 PMID: 16990346

37. Tahmasebi E, Alikhani M, Yazdanian A, Yazdanian M, Tebyanian H, Seifalian A. The current markers of cancer stem cell in oral cancers. Life Sci. 2020; 249: 117483. https://doi.org/10.1016/j.lfs.2020.117483 PMID: 32135187

38. Chou MY, Hu FW, Yu CH, Yu CC. Sox2 expression involvement in the oncogenicity and radiochemoresistance of oral cancer stem cells. Oral Oncol. 2015; 51: 31–39. https://doi.org/10.1016/j.oraloncology.2014.10.002 PMID: 25456004

39. Müller S, Sindikubwabo F, Cañeque T, Lafon A, Versini A, Lombard B, et al. CD44 regulates epigenetic plasticity by mediating iron endocytosis. Nat Chem. 2020. https://doi.org/10.1038/s41557-020-0513-5 PMID: 32747755

40. Adnan Y, Ali SMA, Farooqui HA, Kayani HA, Idrees R, Awan MS. High CD44 Immunoexpression Correlates with Poor Overall Survival: Assessing the Role of Cancer Stem Cell Markers in Oral Squamous

Cell Carcinoma Patients from the High-Risk Population of Pakistan. Int J Surg Oncol. 2022; 2022. https://doi.org/10.1155/2022/9990489 PMID: 35296132

41. Lee SH, Oh SY, Do SI, Lee HJ, Kang HJ, Rho YS, et al. SOX2 regulates self-renewal and tumorigenicity of stem-like cells of head and neck squamous cell carcinoma. British Journal of Cancer 2014 111:11. 2014; 111: 2122–2130. https://doi.org/10.1038/bjc.2014.528 PMID: 25321191

42. Saxena K, Jolly MK, Balamurugan K. Hypoxia, partial EMT and collective migration: Emerging culprits in metastasis. Transl Oncol. 2020; 13. https://doi.org/10.1016/j.tranon.2020.100845 PMID: 32781367

43. Wu F, Ye X, Wang P, Jung K, Wu C, Douglas D, et al. Sox2 suppresses the invasiveness of breast cancer cells via a mechanism that is dependent on Twist1 and the status of Sox2 transcription activity. BMC Cancer. 2013; 13: 1–11. https://doi.org/10.1186/1471-2407-13-317/FIGURES/5

44. Li X, Xu Y, Chen Y, Chen S, Jia X, Sun T, et al. SOX2 promotes tumor metastasis by stimulating epithelial-to-mesenchymal transition via regulation of WNT/β-catenin signal network. Cancer Lett. 2013; 336: 379–389. https://doi.org/10.1016/J.CANLET.2013.03.027 PMID: 23545177

45. Grubelnik G, Boštjančič E, Grošelj A, Zidar N. Expression of NANOG and Its Regulation in Oral Squamous Cell Carcinoma. Biomed Res Int. 2020;2020. https://doi.org/10.1155/2020/8573793 PMID: 32733958

46. Buchakjian MR, Ginader T, Tasche KK, Pagedar NA, Smith BJ, Sperry SM. Independent Predictors of Prognosis Based on Oral Cavity Squamous Cell Carcinoma Surgical Margins. Otolaryngol Head Neck Surg. 2018; 159: 675–682. https://doi.org/10.1177/0194599818773070 PMID: 29737907

47. Züllig L, Roessle M, Weber C, Graf N, Haerle SK, Jochum W, et al. High sex determining region Y-box 2 expression is a negative predictor of occult lymph node metastasis in early squamous cell carcinomas of the oral cavity. Eur J Cancer. 2013; 49: 1915–1922. https://doi.org/10.1016/j.ejca.2013.01.005 PMID: 23414798

48. de Vicente JC, Del Molino PDP, Rodrigo JP, Allonca E, Hermida-Prado F, Granda-Díaz R, et al. SOX2 Expression Is an Independent Predictor of Oral Cancer Progression. Journal of Clinical Medicine 2019, Vol 8, Page 1744. 2019; 8: 1744. https://doi.org/10.3390/jcm8101744 PMID: 31640140

49. Herreros-Villanueva M, Zhang JS, Koenig A, Abel E v., Smyrk TC, Bamlet WR, et al. SOX2 promotes dedifferentiation and imparts stem cell-like features to pancreatic cancer cells. Oncogenesis. 2013;2. https://doi.org/10.1038/oncsis.2013.23 PMID: 23917223

50. Pan X, Cang X, Dan S, Li J, Cheng J, Kang B, et al. Site-specific Disruption of the Oct4/Sox2 Protein Interaction Reveals Coordinated Mesendodermal Differentiation and the Epithelial-Mesenchymal Transition. J Biol Chem. 2016; 291: 18353–18369. https://doi.org/10.1074/jbc.M116.745414 PMID: 27369080

51. Yang N, Hui L, Wang Y, Yang H, Jiang X. SOX2 promotes the migration and invasion of laryngeal cancer cells by induction of MMP-2 via the PI3K/Akt/mTOR pathway. Oncol Rep. 2014; 31: 2651–2659. https://doi.org/10.3892/or.2014.3120 PMID: 24700142

52. Li X, Xu Y, Chen Y, Chen S, Jia X, Sun T, et al. SOX2 promotes tumor metastasis by stimulating epithelial-to-mesenchymal transition via regulation of WNT/β-catenin signal network. Cancer Lett. 2013; 336: 379–389. https://doi.org/10.1016/J.CANLET.2013.03.027 PMID: 23545177

53. Migita T, Ueda A, Ohishi T, Hatano M, Seimiya H, Horiguchi SI, et al. Epithelial-mesenchymal transition promotes SOX2 and NANOG expression in bladder cancer. Lab Invest. 2017; 97: 567–576. https://doi.org/10.1038/labinvest.2017.17 PMID: 28240746

54. Mani SA, Guo W, Liao MJ, Eaton EN, Ayyanan A, Zhou AY, et al. The epithelial-mesenchymal transition generates cells with properties of stem cells. Cell. 2008; 133: 704–715. https://doi.org/10.1016/j.cell.2008.03.027 PMID: 18485877

55. Lee SH, Oh SY, Do SI, Lee HJ, Kang HJ, Rho YS, et al. SOX2 regulates self-renewal and tumorigenicity of stem-like cells of head and neck squamous cell carcinoma. Br J Cancer. 2014; 111: 2122–2130. https://doi.org/10.1038/bjc.2014.528 PMID: 25321191

56. Bareiss PM, Paczulla A, Wang H, Schairer R, Wiehr S, Kohlhofer U, et al. SOX2 expression associates with stem cell state in human ovarian carcinoma. Cancer Res. 2013; 73: 5544–5555. https://doi.org/10.1158/0008-5472.CAN-12-4177 PMID: 23867475

57. Dogan I, Kawabata S, Bergbower E, Gills JJ, Ekmekci A, Wilson W, et al. SOX2 expression is an early event in a murine model of EGFR mutant lung cancer and promotes proliferation of a subset of EGFR mutant lung adenocarcinoma cell lines. Lung Cancer. 2014; 85: 1–6. https://doi.org/10.1016/j.lungcan.2014.03.021 PMID: 24746758

58. Tirelli G, Hinni ML, Fernández-Fernández MM, Bussani R, Gatto A, Bonini P, et al. Frozen sections and complete resection in oral cancer surgery. Oral Dis. 2019; 25: 1309–1317. https://doi.org/10.1111/odi.13101 PMID: 30933401

59. Bajwa MS, Houghton D, Java K, Triantafyllou A, Khattak O, Bekiroglu F, et al. The relevance of surgical margins in clinically early oral squamous cell carcinoma. Oral Oncol. 2020; 110: 104913. https://doi.org/10.1016/j.oraloncology.2020.104913 PMID: 32711167

60. Colaprico A, Silva TC, Olsen C, Garofano L, Cava C, Garolini D, et al. TCGAbiolinks: an R/Bioconductor package for integrative analysis of TCGA data. Nucleic Acids Res. 2016; 44: e71. https://doi.org/10.1093/nar/gkv1507 PMID: 26704973

61. Chandrashekar DS, Bashel B, Balasubramanya SAH, Creighton CJ, Ponce-Rodriguez I, Chakravarthi BVSK, et al. UALCAN: A Portal for Facilitating Tumor Subgroup Gene Expression and Survival Analyses. Neoplasia. 2017; 19: 649–658. https://doi.org/10.1016/j.neo.2017.05.002 PMID: 28732212

62. Di Sanzo M, Chirillo R, Aversa I, Biamonte F, Santamaria G, Giovannone ED, et al. shRNA targeting of ferritin heavy chain activates H19/miR-675 axis in K562 cells. Gene. 2018. https://doi.org/10.1016/j.gene.2018.03.027 PMID: 29544765

63. Biamonte F, Zolea F, Santamaria G, Battaglia AM, Cuda G, Costanzo F. Human haematological and epithelial tumor-derived cell lines express distinct patterns of onco-microRNAs. Cell Mol Biol (Noisy-le-grand). 2017; 63: 75–85. https://doi.org/10.14715/cmb/2017.63.11.14 PMID: 29208177

64. Tamariz-Amador L-E, Battaglia AM, Maia C, Zherniakova A, Guerrero C, Zabaleta A, et al. Immune biomarkers to predict SARS-CoV-2 vaccine effectiveness in patients with hematological malignancies. Blood Cancer J. 2021; 11. https://doi.org/10.1038/s41408-021-00594-1 PMID: 34907159

65. Di Sanzo M, Aversa I, Santamaria G, Gagliardi M, Panebianco M, Biamonte F, et al. FTH1P3, a Novel H-Ferritin Pseudogene Transcriptionally Active, Is Ubiquitously Expressed and Regulated during Cell Differentiation. PLoS One. 2016; 11: e0151359. https://doi.org/10.1371/journal.pone.0151359 PMID: 26982978

66. Zolea F, Battaglia AM, Chiarella E, Malanga D, De Marco C, Bond HM, et al. Ferritin heavy subunit silencing blocks the erythroid commitment of K562 cells via miR-150 up-regulation and GATA-1 repression. Int J Mol Sci. 2017; 18. https://doi.org/10.3390/ijms18102167 PMID: 29039805

67. Chirillo R, Aversa I, Di Vito A, Salatino A, Battaglia AM, Sacco A, et al. FtH-Mediated ROS Dysregulation Promotes CXCL12/CXCR4 Axis Activation and EMT-Like Trans-Differentiation in Erythroleukemia K562 Cells. Front Oncol. 2020; 10. https://doi.org/10.3389/fonc.2020.00698 PMID: 32432042

68. Battaglia AM, Sacco A, Perrotta ID, Faniello MC, Scalise M, Torella D, et al. Iron Administration Overcomes Resistance to Erastin-Mediated Ferroptosis in Ovarian Cancer Cells. Front Oncol. 2022; 12. https://doi.org/10.3389/fonc.2022.868351 PMID: 35433479

69. Scaramuzzino L, Lucchino V, Scalise S, Lo Conte M, Zannino C, Sacco A, et al. Uncovering the Metabolic and Stress Responses of Human Embryonic Stem Cells to FTH1 Gene Silencing. Cells. 2021; 10. https://doi.org/10.3390/cells10092431 PMID: 34572080

70. di Sanzo M, Cozzolino F, Battaglia AM, Aversa I, Monaco V, Sacco A, et al. Ferritin Heavy Chain Binds Peroxiredoxin 6 and Inhibits Cell Proliferation and Migration. Int J Mol Sci. 2022; 23: 12987. https://doi.org/10.3390/ijms232112987 PMID: 36361777

71. Biamonte F, Santamaria G, Sacco A, Perrone FM, Di Cello A, Battaglia AM, et al. MicroRNA let-7g acts as tumor suppressor and predictive biomarker for chemoresistance in human epithelial ovarian cancer. Sci Rep. 2019; 9. https://doi.org/10.1038/s41598-019-42221-x PMID: 30952937

72. Zolea F, Biamonte F, Battaglia AM, Faniello MC, Cuda G, Costanzo F. Caffeine positively modulates ferritin heavy chain expression in H460 cells: Effects on cell proliferation. PLoS One. 2016; 11. https://doi.org/10.1371/journal.pone.0163078 PMID: 27657916

73. Lobello N, Biamonte F, Pisanu ME, Faniello MC, Jakopin Ž, Chiarella E, et al. Ferritin heavy chain is a negative regulator of ovarian cancer stem cell expansion and epithelial to mesenchymal transition. Oncotarget. 2016; 7: 62019. https://doi.org/10.18632/oncotarget.11495 PMID: 27566559

74. Salatino A, Aversa I, Battaglia AM, Sacco A, Di Vito A, Santamaria G, et al. H-Ferritin Affects Cisplatin-Induced Cytotoxicity in Ovarian Cancer Cells through the Modulation of ROS. Oxid Med Cell Longev. 2019; 2019. https://doi.org/10.1155/2019/3461251 PMID: 31781333

75. Biamonte F, Battaglia AM, Zolea F, Oliveira DM, Aversa I, Santamaria G, et al. Ferritin heavy subunit enhances apoptosis of non-small cell lung cancer cells through modulation of miR-125b/p53 axis. Cell Death & Disease 2018 9:12. 2018; 9: 1–10. https://doi.org/10.1038/s41419-018-1216-3 PMID: 30518922